

# A TRMM PR analysis on a contrast in precipitation characteristics across the Baiu front near Japan for evaluations of CMIP5 models

Chie Yokoyama, Yukari N. Takayabu (AORI, University of Tokyo), and Sachie Kanada (University of Tsukuba)

## 1. Motivations

- Tropics and mid-latitudes have differences in the vertical structure of atmospheric stratification. In the tropics, equivalent potential temperature ( $\theta_e$ ) in the lower troposphere is higher, and the lower-mid troposphere is more convectively unstable (Fig. 1a).
- The Baiu front is found between the tropics and the mid-latitudes near Japan during June-July (Figs. 1a and b).
- Key question:** How different are precipitation characteristics between the south and north sides of the Baiu front?
- It is also important to provide an observational evidence on how rain falls associated with the Baiu front near Japan, which is useful to evaluate the performance of climate models.

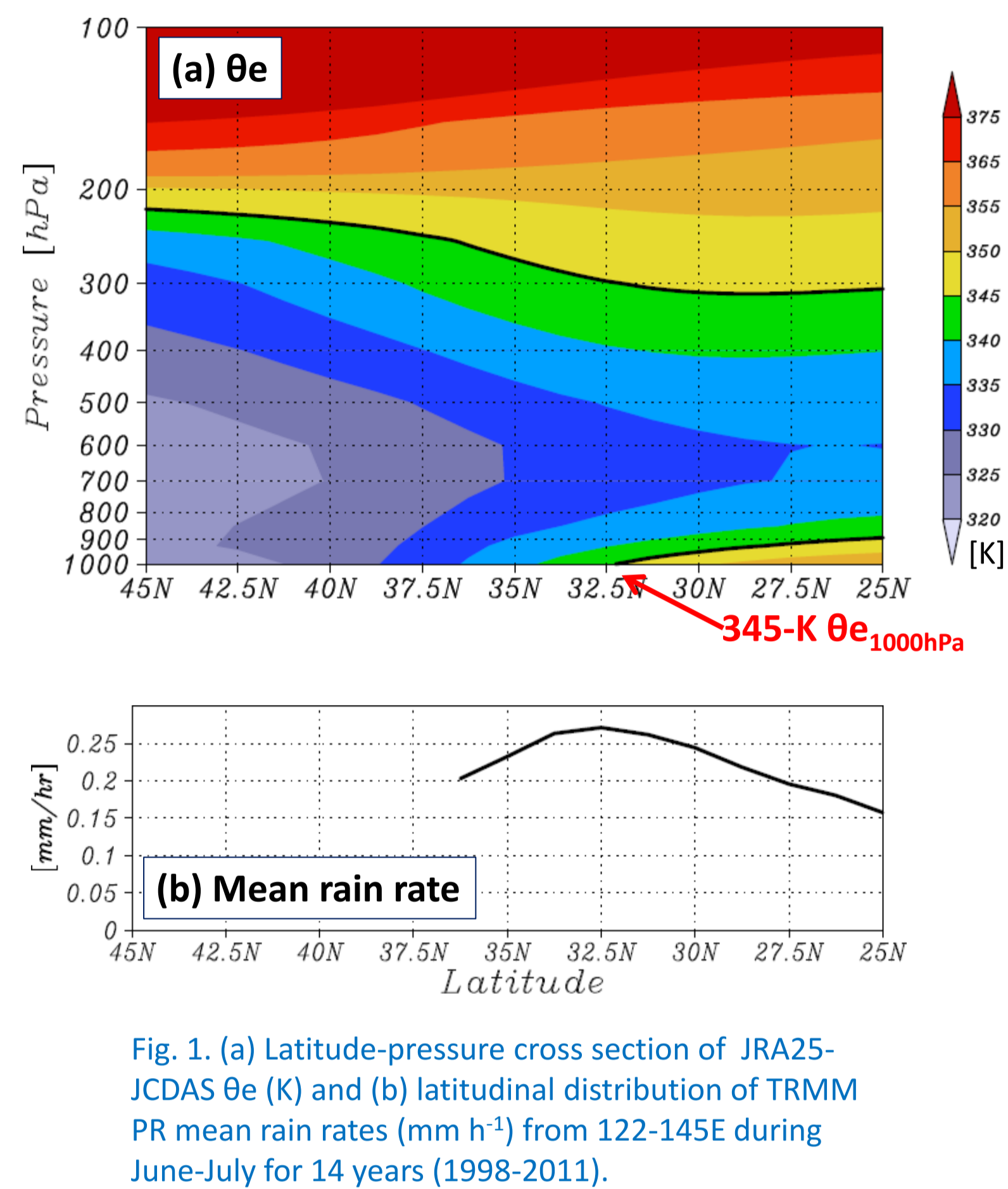
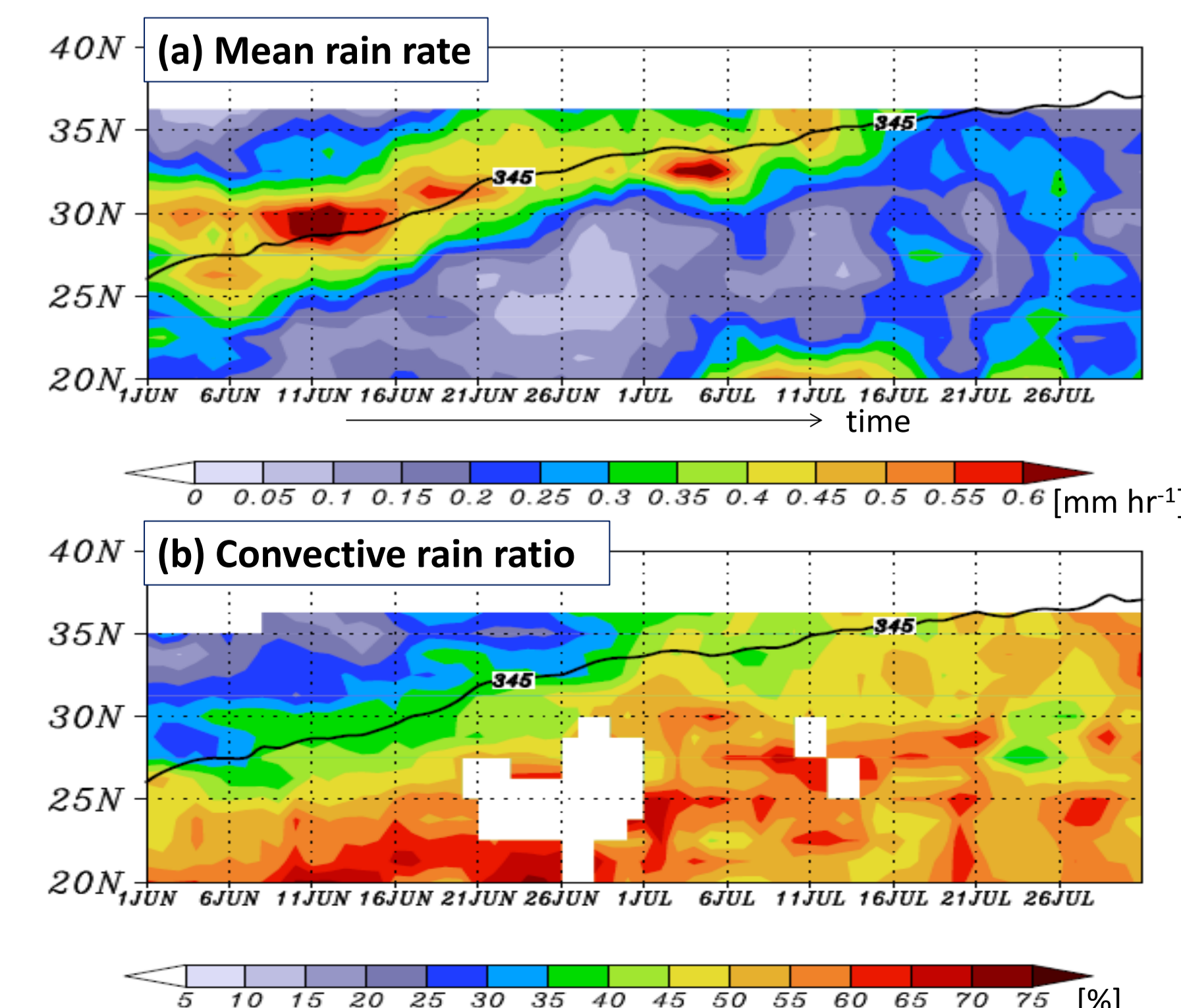


Fig. 1. (a) Latitude-pressure cross section of JRA25-JCDAS  $\theta_e$  (K) and (b) latitudinal distribution of TRMM PR mean rain rates ( $\text{mm h}^{-1}$ ) from 122-145E during June-July for 14 years (1998-2011).

## 2. Data and Methodology

- Data:**
  - TRMM PR2A25 version 7
  - TRMM radar precipitation feature (PF) Level-2 data from University of Utah Database (Liu et al. 2008)
  - JRA25-JCDAS reanalysis data (Onogi et al. 2007)
- Analysis period and longitudes:** June-July from 1998 to 2011 and 122-145° E
- Method:**
  - Define a Baiu front index with 345-K  $\theta_e$  at 1000 hPa ( $\theta_{e,1000\text{hPa}}$ ).
  - Perform composite analysis with its center at latitudes with  $\theta_{e,1000\text{hPa}}$  of 345 K. Reference latitudes are daily determined at every 1.25°.



- The 345-K  $\theta_e$  well corresponds to the migration of the maximum rain rate (Fig. 2a).
- A large increase of **convective rain ratios (CRRs)** is found to the south of the Baiu front index. The boundary that divides precipitation properties moves northward together with the index. (Fig. 2b)

Fig. 2. Time-latitude cross sections of (a) mean mean rain rates ( $\text{mm hr}^{-1}$ ; colors) and (b) convective rain ratios (%) (colors), which are averaged for 14 years (1998-2011). Five-day running mean rain rates for total and convective rain are utilized in this figure. Contours indicate  $\theta_{e,1000\text{hPa}}$  of 345 K. In (b), only regions with at least  $0.1 \text{ mm hr}^{-1}$  are plotted.

## 3. Results

### a) Precipitation characteristics based on pixel data

- On the south side of the reference, convective rain increases compared to the north. **Convective rain ratios (CRRs)** are 40-60% (20-40%) on the south (north). On the south, rain is stronger, and large **rain top heights** more frequently appear (Figs. 1-2).

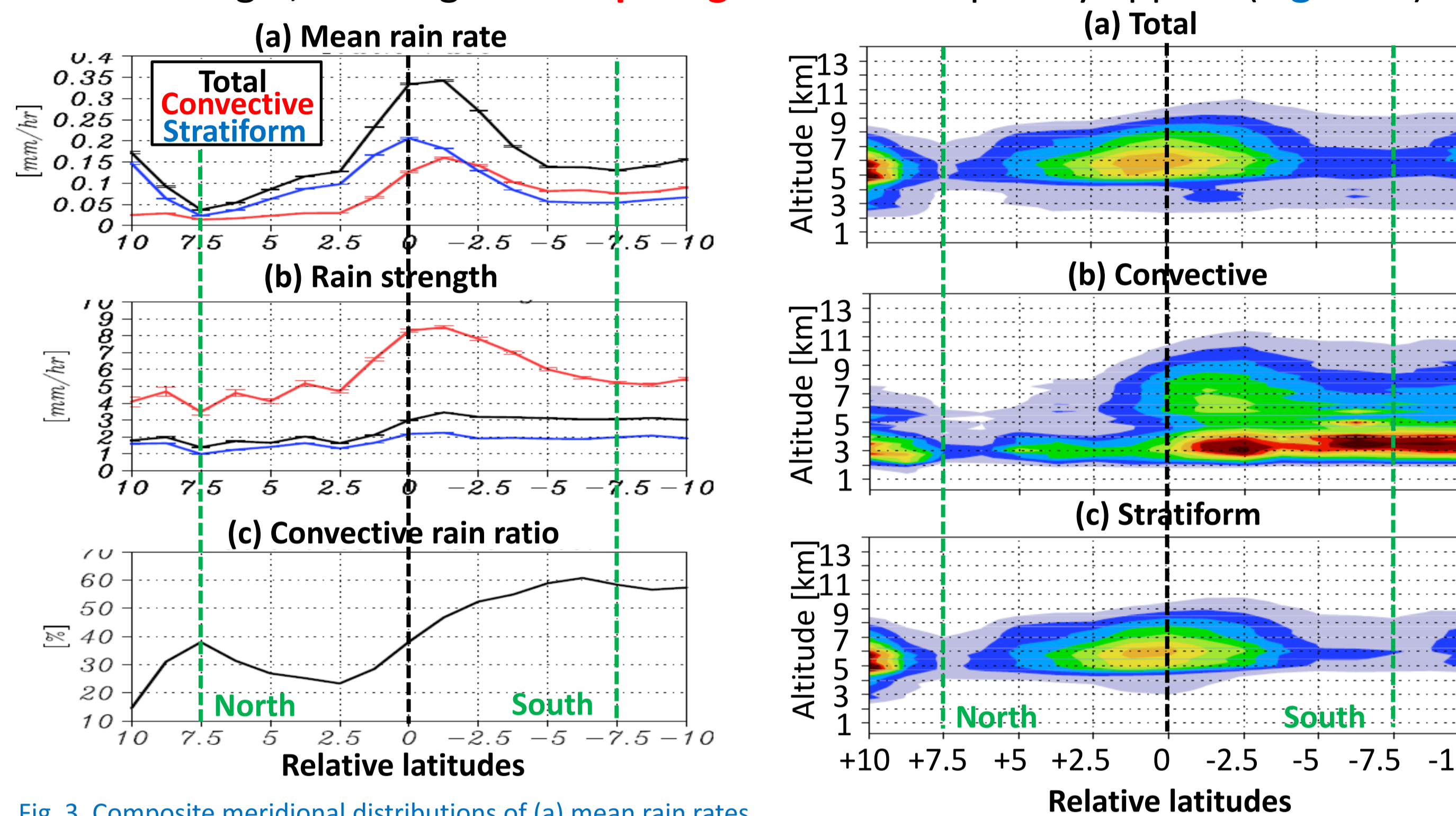


Fig. 3. Composite meridional distributions of (a) mean rain rates, (b) rain strengths, and (c) convective rain ratios. The reference is latitudes with 345-K  $\theta_{e,1000\text{hPa}}$ . In (a) and (b), black, red, and blue lines are for total, convective, and stratiform rain, respectively.

### b) Characteristics of precipitation features (PFs)

- On the south side, PFs with moderate heights (10-14 km) and CRRs of 25-50% and PFs with very large heights (14-18 km) and CRRs of 45-80% are dominant (Figs. 7b and d). These two different types of PFs are similar to **two types of organized systems such as mesoscale convective systems**, which are observed over the tropical Pacific (Yokoyama and Takayabu 2012).
- On the north side, PFs with smaller heights (8-10km) and smaller CRRs (0-40%) have the largest contribution to the total rainfall (Figs. 7a and c).

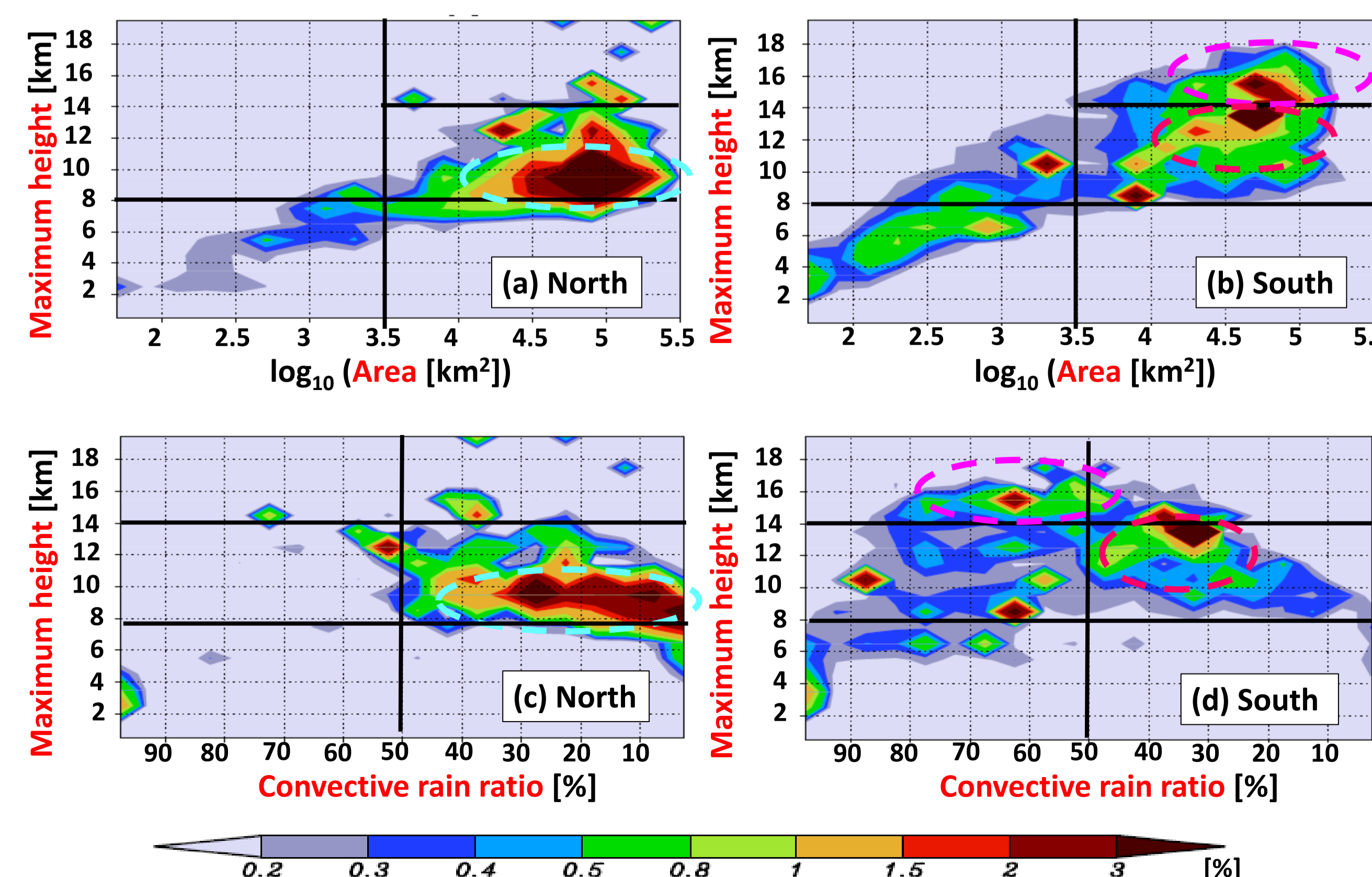


Fig. 7. Composite rain contribution (%) of PFs in terms of (a),(b) areas and maximum 20-dBZ heights, and (c),(d) convective rain ratios and maximum 20-dBZ heights. (a),(c) the north side of the reference ( $0^\circ \sim +7.5^\circ$ ), and (b),(d) the south side ( $-7.5^\circ \sim 0^\circ$ ). In (a) and (b), abscissa indicates PF areas in logarithmic scale.

- Larger effective radar reflectivity factor ( $Z_e$ ) are found at higher altitudes on the south side than the north (Fig. 5). In addition,  $Z_e$  more rapidly decreases above the freezing level on the north.
- For **extreme rain**, rain tops can reach very high altitudes beyond 14 km even on the north side (Fig. 6).

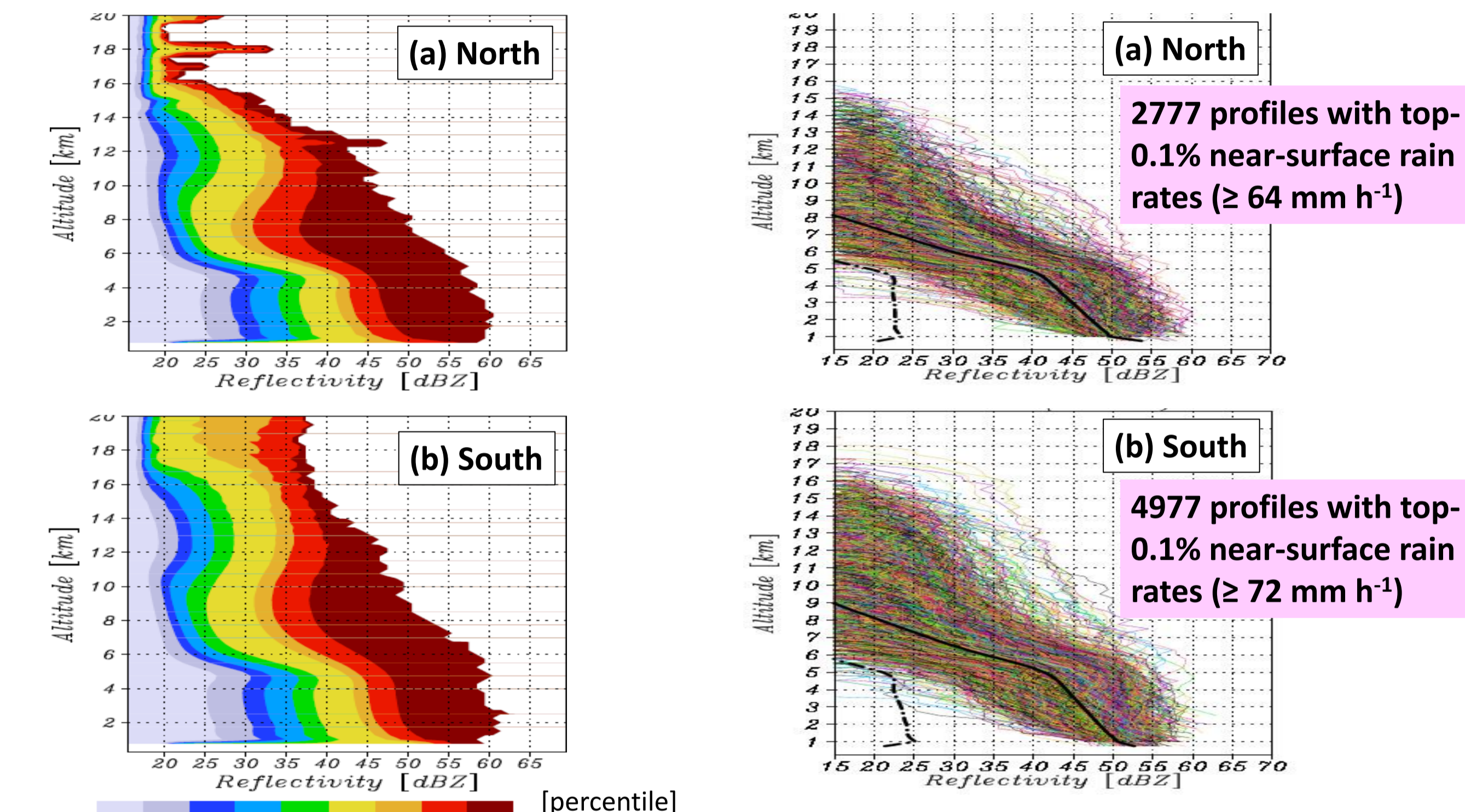


Fig. 4. Composite meridional histograms of rain top heights for (a) total rain, (b) convective rain, and (c) stratiform rain. The reference is latitudes with 345-K  $\theta_{e,1000\text{hPa}}$  of 345 K.

Fig. 5. Composite cumulative frequencies of effective radar reflectivity factor ( $Z_e$ ) by altitudes on the (a) north ( $0^\circ \sim +7.5^\circ$ ) and (b) south ( $-7.5^\circ \sim 0^\circ$ ) sides.

Fig. 6. Ze profiles with extreme near-surface rain rates on the (a) north ( $0^\circ \sim +7.5^\circ$ ) and (b) south ( $-7.5^\circ \sim 0^\circ$ ) sides. Mean  $Z_e$  profiles for all extreme profiles and all observed profiles in each region are plotted with thick black solid and dashed-dotted lines, respectively.

## 4. Summary

- It is shown that there are obvious differences in precipitation characteristics between the south and north sides of the Baiu front. The principal differences are summarized in the following table.

	North side	South side
<b>Convective rain ratio (CRR)</b>	20-40%	40-60%
<b>Rain top height</b>	Smaller	Larger (At the same time, the frequency of shallow convective rain increases.)
<b>Rain strength</b>	Weaker	Stronger
<b>Dominant PFs</b>	PFs with smaller heights (8-10 km) and smaller CRRs (0-40%)	Two types of organized systems; PFs with moderate heights (10-14 km) and CRRs of 25-50%, and PFs with very large heights (14-18 km) and CRRs of 45-80%

- The difference in precipitation regimes on the south and north of the Baiu front is attributed to different characteristics of precipitation systems that are dominant.
- We use this knowledge on the contrast in precipitation characteristics across the Baiu front to evaluate CMIP5 models (not shown in this poster).

**Acknowledgement:** This work is supported by the Environment Research and Technology Development Fund (A-1201) of the Ministry of the Environment, Japan.